

Review

Platinum Group Metal Phosphides as Efficient Catalysts in Hydroprocessing and Syngas-Related Catalysis

Luis Alvarado Rupflin ¹, Chiara Boscagli ² and Stephan Andreas Schunk ^{2,*}

¹ Department of Chemistry, University of Liverpool, Crown Street, Liverpool L69 7ZD, UK; Luis.Alvarado-Rupflin@liverpool.ac.uk

² hte GmbH, Kurpfalzring 104, 69123 Heidelberg, Germany; chiara.boscagli@hte-company.de

* Correspondence: stephan.schunk@hte-company.de; Tel.: +49-6221-7497-0

Received: 23 February 2018; Accepted: 13 March 2018; Published: 20 March 2018

Abstract: Platinum group metal phosphides are reviewed as catalytic materials for hydroprocessing and syngas-related catalysis. Starting from synthetic procedures leading to highly disperse nano-particular compounds, their properties in the applications are discussed and compared with relevant benchmarks, if available. Regarding their mode of action, two confronting mechanistic scenarios are presented: (i) a cooperative scenario in which catalytic sites of different functionalities are active in hydroprocessing and (ii) single site catalysis, which appears to be the relevant mode of action in syngas-related catalysis and which occurs over “frustrated” active sites.

Keywords: platinum group metal phosphides; rhodium phosphide; hydroprocessing; HDS; HDO; carbon monoxide; ethene; propene; hydroformylation

1. Introduction

Transition metal phosphides, although well explored from their solid-state chemistry, are in large parts under-exploited as catalytic materials. The prime focus of research on transition metal phosphides in catalysis was traditionally hydrogenolysis and hydrogenation reactions. Although the phosphide materials in many cases beat traditional benchmarks, up to now industrial applications are limited to nil. Catalysis beyond catalysis involving hydrogen has, up to now, only been sparsely reported; we try to shed light on that aspect by discussing options in syngas-related chemistry. In this review, we try to summarize the major findings for this materials class and, more specifically, for the platinum group metal phosphides, as they stand out for their catalytic properties compared to the other phosphide materials and alternative standards.

2. Structural Discussion of Platinum Group Metal Phosphides

Metals and phosphorus are known to form a large number of crystalline compounds, which display a high variety of metal to phosphorus ratios and a variety of crystalline structures [1]. The ICSD counts 760 entries for binary and 2300 entries for ternary phosphides. As expected, this variety in stoichiometry and structure can also be observed within the binary phosphides of the platinum group metals (PGM), where 23 binary compounds with 16 different structures are reported (Table 1). The phosphides of the PGM, similar to the transition metal phosphides, can be divided into three groups according to the metal to phosphorus ratio [1]:

- polyphosphides (with $n_P > n_M$),
- monophosphides (with $n_P = n_M$),
- metal-rich phosphides (with $n_P < n_M$).

The following review will start with a short overview of some compounds from the three groups, focusing on the phosphides of rhodium since catalytic materials containing rhodium phosphides have the largest amount of reported investigations as materials for catalytic applications in hydroprocessing and syngas-related catalysis. Further overviews of the structure of other binary and ternary metal phosphides can be found in Pöttgen [1], Kuz'ma [2], and Aronsson [3].

Table 1. Overview of the 23 reported binary phosphides, their 16 different structures, and the corresponding space groups of the platinum group metal (PGM) phosphides [1].

Comp.	Structure	Space Group	Ref.	Comp.	Structure	Space Group	Ref.	Comp.	Structure	Space Group	Ref.
RhP ₂	CoSb ₂	P 1 21/c 1	[4]	RuP	MnP	P b n m	[5]	Pd ₁₅ P ₂	Pd ₁₅ P ₂	R -3 H	[6]
IrP ₂	CoSb ₂	P 1 21/c 1	[4]					Pd ₆ P	Pd ₆ P	P 1 21/c 1	[7]
RuP ₂	FeS ₂	P n n m	[8]					Pd _{4,8} P	Fe ₃ C	P n m a	[9]
PdP ₂	NiP ₂	I 1 2/c 1	[10]					Pd ₃ P	Fe ₃ C	P n m a	[11]
PtP ₂	NiP ₂	P a -3	[12]					Pd ₅ P ₂	Fe ₃ C	P n m a	[9]
RhP ₃	CoAs ₃	I m -3	[13]					Pt ₅ P ₂	Pt ₅ P ₂	C 1 2/c 1	[14]
PdP ₃	CoAs ₃	I m -3	[13]					Pd ₇ P ₃	Pd ₇ P ₃	R 3 H	[15]
IrP ₃	CoAs ₃	I m -3	[13]					Ru ₂ P	Co ₂ P	P b n m	[16]
RuP ₃	RuP ₃	P -1	[17]					Rh ₂ P	anti-CaF ₂	F m -3 m	[1,18]
RuP ₄	OsP ₄	P 1 21/c 1	[2,19]					Ir ₂ P	anti-CaF ₂	F m -3 m	[13]
								Rh ₃ P ₂	anti-PbFCl	P -4 m 2	[20]
								Rh ₄ P ₃	Rh ₄ P ₃	P n m a	[21]

The polyphosphides of the PGMs are, as other polyphosphides, characterized by the formation of P–P bonds. The compounds RhP₃, PdP₃, and IrP₃ crystallize in the CoAs₃ structure [13] where the phosphorus atoms are coordinated to octahedrons. Further, the formation of P₄^{−4} rings can be observed (Figure 1e). Other binary polyphosphides crystallize in the pyrite structure and in other related structures. RuP₂ crystallizes in the FeS₂ structure (cubic) [8] and PtP₂ and PdP₂ crystallize in the NiP₂ structure [10,22]. RhP₂ (Figure 1d) and IrP₂ both crystallize in the CoSb₂ structure (monoclinic) [4]. In all three structures the metal coordinates the phosphorus to octahedrons, which are connected to each other by the formation P₂ dimers (Figure 1d).

The only reported monophosphide of the platinum metal group is RuP, which crystallizes in the MnP structure [5], just as the other transition metal phosphides (NiP, MnP). This structure can be distinguished by the formation of phosphorus zigzag chains along the c-axis.

Metal-rich phosphides are characterized by the formation of metal to metal bonds. Certain metal-rich PGM phosphides crystallize in a number of unique structure types compared to other transition metal phosphides that cannot be found in any other phosphide compound (Pd₁₅P₂, Pd₆P, Pt₅P₂, Pd₇P₃, and Rh₄P₃). Ru₂P crystallizes in the Co₂P structure, which is related to the anti-PbCl structure [16]. Characteristic of this structure is the formation of a distorted tetragonal prism ordered in chains along the b-axis (Figure 1f). Rh₂P and Ir₂P crystallize in the anti-CaF₂ structure [1,18]; in this structure, the metal coordinates the phosphorus atoms to tetrahedrons (Figure 1a).

The phosphides of rhodium are among the most investigated compounds of all the PGM phosphides in the field of heterogeneous catalysis. There are five different phosphides of rhodium (Rh₂P, Rh₃P₂, Rh₄P₃, RhP₂, and RhP₃) [23]. The compounds Rh₃P₂ and Rh₄P₃ both crystallize in specific structure types. The Rh₃P₂ structure is characterized by the coordination of the phosphorus to tetrahedrons and square pyramids; planes of tetrahedrons and pyramids are stapled over each other (Figure 1b). In the Rh₄P₃ structure, the phosphorus is coordinated to square pyramids (Figure 1c).

The structures of some rhodium phosphides are isomorphic with some other metal phosphides. The phosphides RhP₃, IrP₃, CoP₃, and NiP₃ all crystallize in the CoAs₃ structure. The phosphides RhP₂, IrP₂, and CoP₂ all crystallize in the CoSb₂ structure (Figure 1f). Finally, the metal-rich phosphides Rh₂P and Ir₂P both crystallize in the anti-CaF₂ structure; up to now, no ternary compounds have been reported. Common to all of the compounds is that with increasing metal to phosphorus ratio, the metallic properties of the phosphides increase. This can be observed especially regarding the distance between the rhodium atoms of the metal-rich rhodium phosphides. The distance between

the rhodium atoms in Rh_4P_3 lies between 0.280 and 0.294 nm, in Rh_3P_2 between 0.282 and 0.285 nm, and in Rh_2P only 0.276 nm [1,3]. This last distance is just slightly larger than the distance between two rhodium atoms in metallic rhodium (0.27 nm).

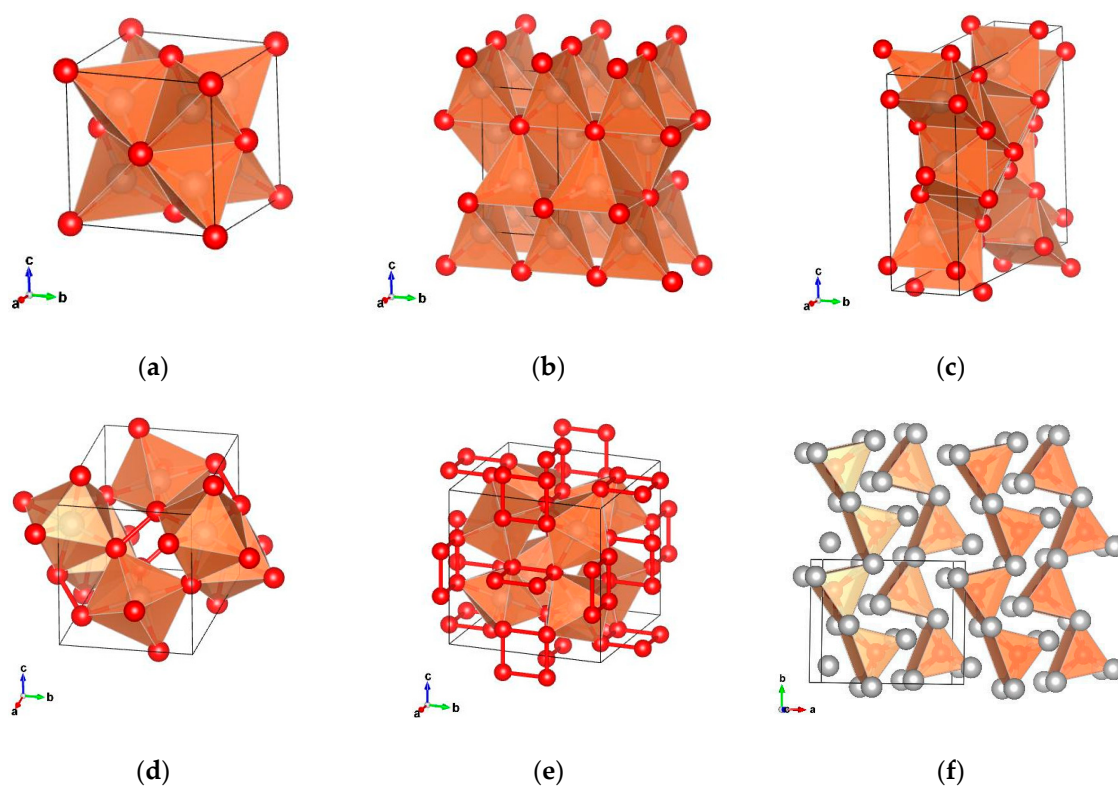


Figure 1. The structure of selected platinum group metal (PGM) phosphides. The metal atoms are displayed in grey and the phosphorus atoms in red. (a) Rh_2P crystallizes in the anti- CaF_2 structure; (b) Rh_2P_3 ; (c) Rh_4P_3 ; (d) RhP_2 crystallizes in the CoSb_2 structure forming P_2 dimers; (e) RhP_3 crystallizes in the CoAs_3 structure forming Rh_4^{-4} rings; (f) the Co_2P structure with chains of slightly distorted prisms.

3. Synthetic Pathways to Supported Platinum Group Metal Phosphides

As platinum metals are scarce and per unit mass expensive, the application of bulk materials for any application of commercial relevance can only have model character. A number of groups have embarked on developing ways to support nanoparticles of PGM phosphides. A variety of pathways for the preparation of transition and platinum group metal phosphides, either as a bulk material or as a support material for catalysis applications, have been reported. An overview of the different preparation pathways has been given by Aronsson et al. [3], Kuz'ma et al. [2,4], Pöttgen et al. [1], Prins et al. [5,24] and Oyama et al. [25,26]. Aronsson, Kuz'ma, and Pöttgen described the preparation of bulk binary and ternary phosphides and their structure while Prins and Oyama focused mainly on the preparation of supported transition metal phosphides for catalysis applications.

The three routes to be described next are the most frequently reported pathways in the literature for the preparation of supported platinum group metal phosphides:

- the incipient wetness impregnation method combined with reductive treatment,
- the conversion of supported metals or metal oxides with a phosphorus-containing compound combined with reductive treatment,
- the deposition of metal phosphide nanoparticles prepared via colloidal preparation routes on a support material.

Figure 2 gives a schematic overview of the three pathways and Table 2 lists different supported PGM phosphides, the pathways by which they are prepared, and the relevant references from the literature.

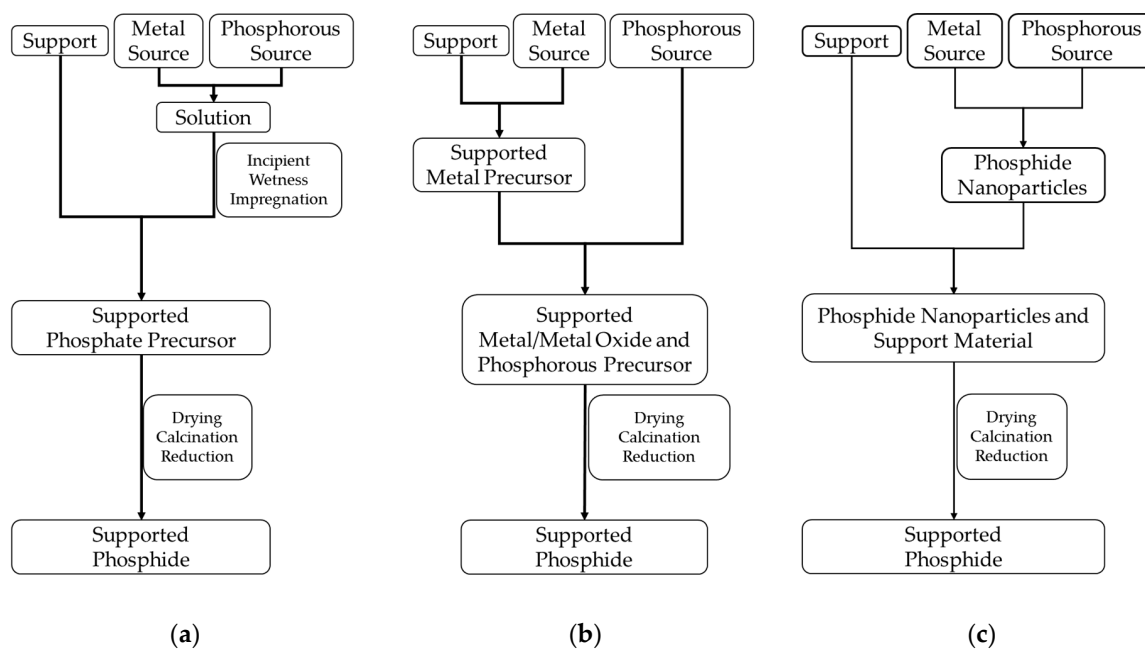


Figure 2. Schematic for the three main synthetic pathways for supported PGM phosphides: (a) Method of the incipient wetness impregnation; (b) Method of the conversion of a supported metal or metal oxide with a phosphorus precursor; (c) Method of the deposition of phosphide nanoparticles on the support material.

The incipient wetness impregnation method (Figure 2a) consists in the preparation of a supported metal phosphate precursor that is then heated under a reductive atmosphere (H_2 or minor amounts of H_2 in N_2) to form the metal phosphide. First, the support material is impregnated with a solution containing the metal and phosphorus precursor. Nitrates and chlorides of the metals and $(NH_4)_2HPO_4$ are the most commonly used precursors. The samples are dried after the impregnation and further fired under air to decompose the nitrate or chloride compounds and to form the oxide and phosphate precursors. Last, the sample is reduced under hydrogen-containing atmosphere to form the corresponding phosphides.

The incipient wetness impregnation method combined with reductive treatment can be applied to prepare a broad range of metal phosphides, metal to phosphorus ratios (mainly metal-rich phosphides), and support materials for the preparation of dispersed PGM phosphides.

Hayes et al. [27] applied the incipient wetness impregnation for the preparation of Rh_2P on SiO_2 for the hydrodesulfurization (HDS) of thiophen with a rhodium (Rh) loading of 5 wt %. First, a solution of $RhCl_3 \cdot xH_2O$ and $NH_4H_2PO_4$ with an Rh:P = 1 in ultra-pure water is prepared and impregnated on the support material SiO_2 , followed by a drying step at 318 K, calcination at 773 K, and reduction at 923 K under pure H_2 flow. The characterization via XRD shows the formation of Rh_2P without metallic Rh impurities. TEM investigations show well dispersed Rh_2P particles with an average size of approximately 5 nm.

Habas et al. [28] applied the method of the incipient wetness impregnation, among others, for the preparation of Rh_2P and Pd_3P on SiO_2 in order to compare the performance of the samples prepared by the different pathways as catalysts for the hydrodeoxygenation (HDO) of acetic acid as a model compound. Kanda et al. [6,29] applied the incipient wetness impregnation method for the preparation of Ru_2P , PtP_2 , Rh_2P , and $Pd_{4.8}P$ on SiO_2 to test the metal phosphides as catalysts in the HDS of

thiophen. On later publications, Kanda et al. [30] focused on the preparation of Rh_2P on different support materials (SiO_2 , TiO_2 , Al_2O_3 , MgO , and ZrO_2) and the effect of the reduction temperature and the effect of phosphorus loading [31] on the formation of Rh_2P . The compound Rh_2P can be successfully prepared on all the support materials investigated. Further, Kanda observed the formation of Rh_2P on SiO_2 at lower reduction temperatures ($350\text{ }^\circ\text{C}$) with a high excess of phosphorus ($\text{P}:\text{Rh} = 2$), while higher temperatures are required ($550\text{ }^\circ\text{C}$) to form phase-pure Rh_2P on SiO_2 samples with a lower excess of phosphorus ($\text{P}:\text{Rh} = 1$). This shows that the addition of P enhances the formation of Rh_2P at lower temperatures, but an excess of P leads to the formation of RhP_2 at higher reduction temperatures. Further, the TEM investigation shows that the average particle diameter of the Rh_2P particles on the catalysts increases with increasing reduction temperature and P content. A sample reduced at $550\text{ }^\circ\text{C}$ with 1.5 wt % P loading has an average particle diameter of 6.4 nm, while a sample with 3.0 wt % has an average particle diameter of 8.8 nm. Kanda et al. [32] also compared the use of acetylacetonato (acac) precursors and triphenylphosphine (TPP) with the use of chloride and phosphate precursors for the preparation of Rh_2P and $\text{Pd}_{4.8}\text{P}$ on SiO_2 . When the acac precursor and TPP are employed, slightly lower reduction temperatures are needed for the formation of the phosphides. In the PXRD patterns, the group observed phase-pure Rh_2P on SiO_2 at a reduction temperature of $450\text{ }^\circ\text{C}$ when the acac and TPP precursors are used, while a temperature of $650\text{ }^\circ\text{C}$ is needed when chloride and phosphate are used as precursors.

Sawada et al. [33,34] prepared Rh_2P catalysts supported on SiO_2 , Al_2O_3 , and different zeolites (Na-beta, Na-MFI, Na-MOR) for the HDS of thiophen via the incipient wetness impregnation method. Sawada et al. [33] investigated the effect of Na doping on the formation of Rh_2P . The addition of Na to samples lowers the required reduction temperature of the samples supported on zeolites or Al_2O_3 by weakening the interactions between the Al and the phosphate precursor [33].

Alvarado et al. [35] applied the incipient wetness method for the preparation of Rh_2P on SiO_2 and investigated the effect of the reduction temperature on the performance of the samples in the hydroformylation of ethene and propene. XRD patterns show the formation of phase-pure Rh_2P at temperatures of $500\text{ }^\circ\text{C}$ that remain stable at temperatures of $900\text{ }^\circ\text{C}$. TEM images reveal a slight increase in the particle size by increasing the reduction temperature from 250 to $900\text{ }^\circ\text{C}$. Further, HRTEM analysis of a single particle from the sample reduced at $900\text{ }^\circ\text{C}$ reveals high crystallinity of Rh_2P with cubic structure.

Guan et al. [36] and Wang et al. [37] also applied the method of the incipient wetness for the preparation of supported RuP and Ru_2P on MCM-41 and on SiO_2 , respectively. Guan used $\text{RuCl}_3 \cdot 3\text{H}_2\text{O}$ and $\text{NaH}_2\text{PO}_4 \cdot \text{H}_2\text{O}$ as precursors for the incipient wetness impregnation and a static Ar environment for the thermal treatment of the samples. From the results, Guan proposed a mechanism for the formation of the phosphides: first, PH_3 is formed by the decomposition of NaH_2PO_4 , which reduces RuCl_3 to Ru. Further formation of PH_3 allows Ru to form Ru_2P or RuP , depending on the amount of PH_3 present.

Wang et al. [37] compared two similar preparation methods: the conventional method, which implies the use of RuCl_3 and $\text{NH}_4\text{H}_2\text{PO}_4$ as precursors for the incipient wetness impregnation; and a new method applying RuCl_3 and triphenylphosphine (TPP) dissolved in ethanol for a slurry impregnation. Both compounds, RuP and Ru_2P , can be prepared with the two methods by modifying the metal to phosphorus ratios; however, lower reduction temperatures are needed for the formation of the phosphide when TPP is used.

Later publications investigated the doping of Ni_2P with noble metals such as Ir, Rh, Ru, and Pt on SiO_2 [7,38] or Zeolites [39]. The groups applied the method of the incipient wetness, preparing first a solution with the two metals and the phosphorus precursor and impregnating it on the support material, followed by a drying, calcination, and reduction step. XRD patterns show the formation of Ni_2P with no impurities.

A further synthetic pathway for the preparation of supported metal phosphides consists of the conversion of supported metals or metal oxides with a phosphorus precursor to the corresponding phosphides (Figure 2b).

First, the preparation of a supported metal or metal oxide takes place. This can be carried out, for example, via incipient wetness of the support material with a solution of the metal precursor, followed by a calcination step and subsequent reduction to obtain the supported metal. For the preparation of the phosphides, a phosphorus precursor is added to the supported metal or metal oxide followed by a thermal treatment.

Muetterties et al. [40] described this method in 1974 for the preparation of the phosphides of Ru, Rh, Pd, Pt, and other transition metals (Ni, W, Co, Fe) on Al_2O_3 . First, the metal or metal oxides are prepared on the support material. The supported metals and metal oxides are then treated under a mixture of He and PH_3 in a temperature range of 250–300 °C to form the phosphides. Unfortunately, the materials were not characterized by XRD to confirm the formation of the phases.

Bowker et al. [41] prepared first RuO_4 and PdO on SiO_2 , which is then impregnated with $\text{NH}_4\text{H}_2\text{PO}_2$ and heated to 700 °C under a H_2 atmosphere for the formation of the phosphides. By changing the phosphorus to metal ratio during the preparation, the phosphides RuP or Ru_2P and Pd_5P_2 or Pd_3P can be prepared.

Kucernak et al. [42] used commercial Pd on active carbon, which is then heated in trioctylphosphine (TOP) to 300 °C for the formation of Pd_5P_2 and PdP_2 . A similar method was applied by Kanda et al. [43] for the preparation of Rh_2P on Al_2O_3 . First, Rh on Al_2O_3 is prepared via incipient wetness impregnation, calcination, and reduction. The Rh on Al_2O_3 is impregnated with a TPP/hexane solution, dried under inert conditions, and reduced under a 5% H_2 in N_2 flow at different temperatures. Kanda also prepared a further catalyst using the $(\text{NH}_4)_2\text{HPO}_4$ to compare the reduction temperature of the two samples. By using TPP as a phosphorus precursor instead of using a phosphate precursor, the reduction temperature for the formation of the phosphide can be decreased from 800 to 650 °C.

The last method discussed here consists in the deposition of phosphide nanoparticles, prepared via colloidal methods, on the support material (Figure 2c). First, the platinum group metal phosphide nanoparticles are prepared and, on a second step, deposited on the support material. The preparation of the nanoparticles beforehand seems to allow better control of the size and size distribution of the PGM phosphides. The preparation of phosphide nanoparticles can be carried out by preparing first the metal nanoparticles and then reacting them with PH_3 [44]. Another highly reactive possible phosphorus precursor is $\text{P}(\text{SiMe}_3)_3$, which allows a one-pot preparation of the phosphide nanoparticles and has been successfully applied for the preparation of Ni_2P nanoparticles. A further, less reactive but versatile and more and more common phosphorus precursor for the preparation of phosphide nanoparticles is TOP. Carenco et al. [44] reviewed the preparation of nano-scaled metal phosphides where they reported the development of the synthetic pathways from highly active precursors such as PH_3 and metal carbonyls to more stable ones such as TOP and metal acetylacetonates. Henkes et al. [45] showed the versatility of TOP as a phosphorus precursor using it for the preparation of different metal phosphides (Cu, Fe, Ni, Co, Ag, In, Rh, Pd, Zn) as nanoparticles, powder, foils, wires, and thin films. Henkes et al. [46] also prepared Rh nanoparticles with different shapes and morphologies and converted them to Rh_2P using TOP. The phosphides keep the same shape as the metal templates, as shown on TEM images. A further method for the preparation of phosphide nanoparticles is the use of single-source molecular precursors such as $\text{Ni}(\text{PPh}_3)_2(\text{CO})_2$, $\text{Rh}(\text{PPh}_3)_2(\text{CO})\text{Cl}$, or $\text{Pd}(\text{PPh}_3)_4$, mixed in oleylamine and 1-octadecene, heated to 300 °C for 1 h and cooled to room temperature. The nanoparticles are then washed with ethanol and centrifuged. Single-source precursors were used by Habas et al. [28] and by Griffin et al. [47] for the preparation of Ni_2P , Rh_2P , and Pd_3P on SiO_2 . The Rh_2P nanoparticles are formed using $\text{Rh}(\text{PPh}_3)_2(\text{CO})\text{Cl}$ mixed in an oleylamine and 1-octadecene solution, which is heated up to 300 °C. The nanoparticles are recovered, washed with ethanol, re-dispersed in CHCl_3 , and added to a suspension of SiO_2 in CHCl_3 , sonicated and dried to form the finished catalyst.

Table 2. Overview of the methods applied for the preparation of supported phosphides.

Method	Compound	Support	Ref.
Incipient wetness impregnation	Pd ₃ P	SiO ₂	[28]
	Pd _{4,8} P	SiO ₂	[6,29]
	Rh ₂ P	La ₂ O ₃ /Al ₂ O ₃	[48]
		SiO ₂	[27–31,33,35]
		TiO ₂	[30]
		Al ₂ O ₃	[30,33]
		MgO	[30]
		ZrO ₂	[30]
		MFI	[33]
		Na-Beta	[34]
		Na-MFI	[34]
		Na-MOR	[34]
		RuP	MCM-41
	Ru ₂ P	SiO ₂	[37]
		MCM-41	[36]
		SiO ₂	[37]
Conversion of a supported metal or metal oxide precursor	Pd ₃ P	SiO ₂	[41]
	Pd ₅ P ₂	SiO ₂	[41]
		Active Carbon	[42]
	PdP ₂	Active Carbon	[42]
	Rh ₂ P	Al ₂ O ₃	[43]
	Ru ₂ P	SiO ₂	[41]
	RuP	SiO ₂	[41]
Deposition of nanoparticles	Pd ₃ P	SiO ₂	[28]
	Rh ₂ P	SiO ₂	[28,47]

4. Rh₂P as a Prototypic Example for PGM Phosphides in Hydrotreating Reactions

Of all the rhodium phosphides, only Rh₂P has been reported to be a suitable catalyst material for different reactions, mainly the HDS and HDO of hydrocarbons. Most of the investigations regarding the application of metal phosphides in hydrotreating reactions have been driven by the motivation to find improved hydrotreating catalysts due to the increasing environmental regulations limiting the content of sulfur in transportation fuels and due to the diminishing quality of oil feedstocks [25,26,49]. The most investigated metal phosphide is Ni₂P [24–26,49], which shows high activity in the HDS of dibenzothiophene (DBT) where it hydrogenates preferably the sulfur compound than the aromatic ring [8,50]. The activity of the Ni₂P catalysts supported on SiO₂ is comparable to the activity of a commercially available Ni-Mo-S/Al₂O₃ catalyst. Further investigations show the higher activity of CoP for the HDN of chinolin [50], of MoP and Ni₂P for the HDO of palmitic acid [51], or Ni₂P for the HDO of benzofuran [50]. Within the frame of these investigations, different PGM phosphides have been tested as catalyst materials. Here, the Rh₂P/SiO₂ material shows a significantly higher activity in the HDS of DBT than Rh/SiO₂ and higher than the Ni₂P/SiO₂ material [27]. Further investigations have shown that Rh₂P has a higher activity in the HDS of thiophene than all the other PGM phosphides [29]. Due to the higher intrinsic activity of the Rh₂P catalyst, different publications have focused on the application of Rh₂P as a catalyst material for hydrotreating reactions [27–34,43,47,52], for the hydrogen evolution reaction [53], and for the hydroformylation [35]. Reviews focusing on the metal phosphides in general and their applications as catalyst materials can be found elsewhere [24–26,49,54,55].

The next section of this review deals with the application of Rh₂P as a catalyst material for the reactions of HDS and HDO. Investigations regarding the application of Rh₂P as a catalyst for the HDN have not been published yet to our knowledge.

4.1. Rh₂P as a Catalyst Material for HDS

Among the first investigations on the application of Rh₂P as a catalyst material in HDS are the articles published by Hayes et al. [27] who prepared a series of supported Rh-based catalysts (Rh₂P, Rh, sulfonated Rh on SiO₂, Rh loading of 5 wt %) and compared their performance in the HDS of DBT. The findings of their investigation show that the Rh₂P/SiO₂ catalyst material is more active in the HDS of DBT (fixed-bed reactor, temperature range of 225–300 °C, 3.0 MPa, Feed: decalin solution with 3000 ppm DBT) than the sulfonated Rh/SiO₂ and the Rh/SiO₂ catalysts; and is also more active than the commercially available Ni-Mo/Al₂O₃ catalyst used as a benchmark, as shown on Figure 3a. Table 3 shows the results of the investigation at 275 °C where Rh₂P/SiO₂ shows significantly higher conversion values (99.0%) than the benchmark catalyst Ni-Mo/Al₂O₃ (84.2%). The product distribution shows that the Rh₂P/SiO₂ catalyst favors the hydrogenation of the first aromatic ring and then the removal of S, and thus the high selectivity values for cyclohexane–benzene.

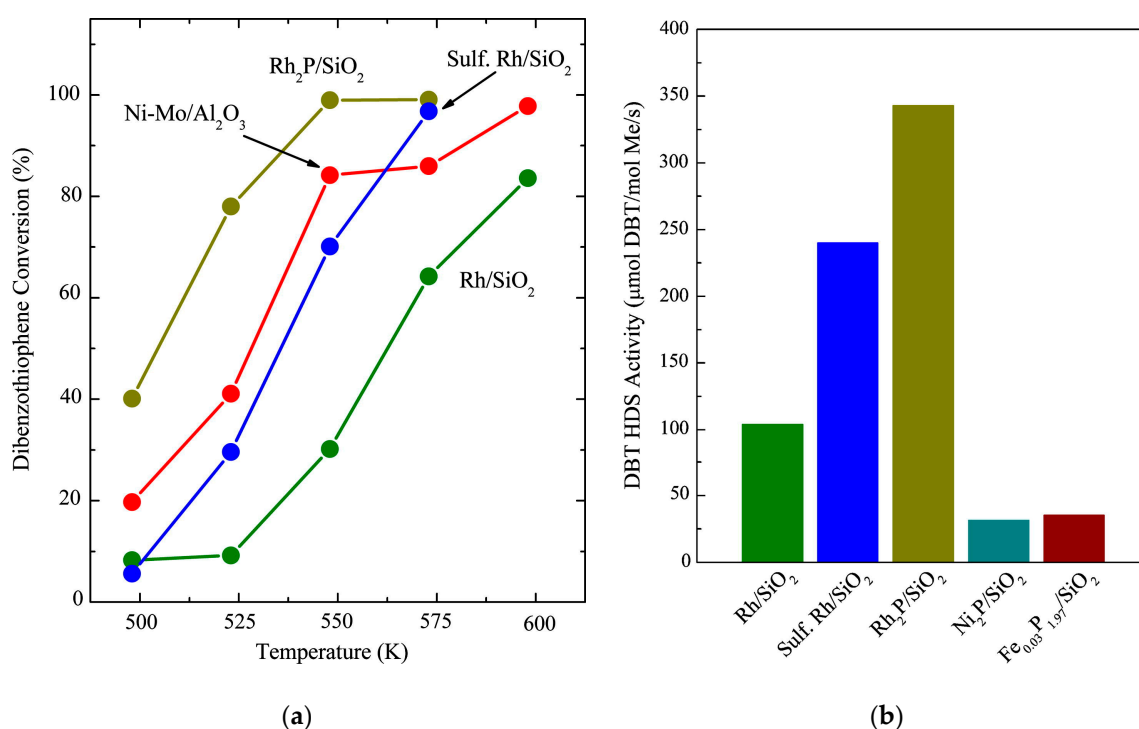


Figure 3. Results of the catalyst testing by Hayes et al.: (a) Performance of the different catalyst materials; (b) Normalized dibenzothiophene (DBT) activity of different catalyst materials. Printed with permission of [27].

Table 3. Comparison of the performance of different catalysts in the hydrodesulfurization (HDS) of dibenzothiophene (DBT) in the investigation of Hayes et al. [9] (275 °C, 3.0 MPa, 3000 ppm HDS in decalin).

Catalyst	Conversion	BP ¹	CHB ²	BCH ³
Rh ₂ P/SiO ₂	99.0	4.1	52.1	43.8
Sulf. Rh/SiO ₂	70.1	52.7	46.1	1.2
Rh/SiO ₂	30.2	77.0	18.9	4.1
Ni-Mo/Al ₂ O ₃	84.2	66.2	30.8	3.0

¹ BP: 4,4'-Biphenyl; ² CHB: Cyclohexylbenzene; ³ 1,1'-Bi(cyclohexyl).

Further findings of the investigation are the higher tolerance of the Rh₂P catalyst toward H₂S than the Rh/SiO₂ catalyst. Both materials were tested before and after co-feeding of 50 kPa H₂S. The conversion of DBT at 275 °C decreases from 80% to 22% for the Rh₂P catalyst and from 65% to 12% for the Rh/SiO₂ catalyst. The normalization of the HDS activity per mol of metal allowed the authors to make a comparison with other catalyst systems such as a 25 wt % Ni₂P/SiO₂ catalyst. Hayes et al. showed that the per mol metal HDS activity of the Rh₂P/SiO₂ catalyst at 275 °C is approx. eleven times higher than the activity of the Ni₂P/SiO₂ catalyst, as Figure 3b and the values in Table 4 show, and so increasing the interest in Rh₂P as a suitable catalyst material for the HDS reaction.

Table 4. Normalized HDS activity of different catalyst materials (275 °C, 3.0 MPa, 3000 ppm DBT in decalin) [9].

Catalyst	HDS Activity [$\mu\text{mol DBT/mol Me/s}$]
Rh ₂ P/SiO ₂	330.4
Sulf. Rh/SiO ₂	241.0
Rh/SiO ₂	102.9
Ni ₂ P/SiO ₂	32.5
Fe _{0.03} P _{1.97}	35.2

Most of the work performed on Rh₂P as a hydrogenolysis active catalyst material for the HDS reaction has been reported by the group of Yasuharu Kanda. In a first publication [29], the performance of PGM metals and PGM phosphides supported on SiO₂ (Rh₂P, Pd_{4.6}P, Ru₂P, and PtP₂) were compared in the HDS reaction of thiophene. The findings of the investigation are that the Rh₂P/SiO₂ catalyst is the most active PMG phosphide in the HDS of thiophene, as shown by the results in Table 5 and Figure 4. The Rh₂P/SiO₂ catalyst shows the highest values for the conversion of thiophene in the HDS reaction. Further findings are that Rh₂P/SiO₂ is more active than the Ni₂P/SiO₂ catalyst; that Rh₂P/SiO₂ has a comparable activity to the commercial CoMoP/Al₂O₃ catalyst they use as a benchmark; that the PGM phosphides are superior to the PGMs themselves and, therefore, phosphide formation is essential for the activity of the material, as shown in the results in Table 5. The Rh/SiO₂ catalyst achieves a conversion value of 13.32% while Rh₂P/SiO₂ achieves a value of 54.95%; the only phosphide displaying a lower activity than the metal is PtP₂.

Table 5. Performance of different PMG metals and phosphides in the HDS of thiophene (fixed-bed reactor, 0.1 g catalyst, 350 °C, 0.1 MPa, H₂/thiophene = 30, W/F = 37.9 g h mol⁻¹) [29].

Catalyst	Reduction Temperature [°C]	Conversion [%]	C ₁ -C ₃	Butanes	Butene	1,3-Butadiene	THT ¹
Rh/SiO ₂	450	13.32	12.13	85.28	0.00	2.59	12.13
Rh ₂ P/SiO ₂	550	54.95	20.82	75.54	0.00	3.53	20.82
Pd/SiO ₂	350	39.86	26.96	70.38	0.00	2.66	26.96
Pd _{4.8} P/SiO ₂	500	45.85	10.04	87.48	0.00	1.42	10.04
Ru/SiO ₂	350	0.28	0.00	77.81	22.19	0.00	0.00
Ru ₂ P/SiO ₂	650	12.66	4.94	86.85	0.00	8.21	4.94
Pt/SiO ₂	400	22.09	52.05	41.48	0.00	6.47	52.05
PtP ₂ /SiO ₂	650	3.36	14.25	60.15	0.00	25.60	14.25
CoMoP/Al ₂ O ₃	400	53.28	18.67	80.53	0.00	0.10	18.67

¹ THT: tetrahydrothiophene.

In investigations concerning the reaction mechanism, it was proven that direct desulfurization is favored over dehydrogenation of the double bonds of thiophene (reaction route 1 on Figure 5). The product with the highest selectivity is 1-butene, followed by butane and small amounts of tetrahydrothiophene, as seen in Table 5.

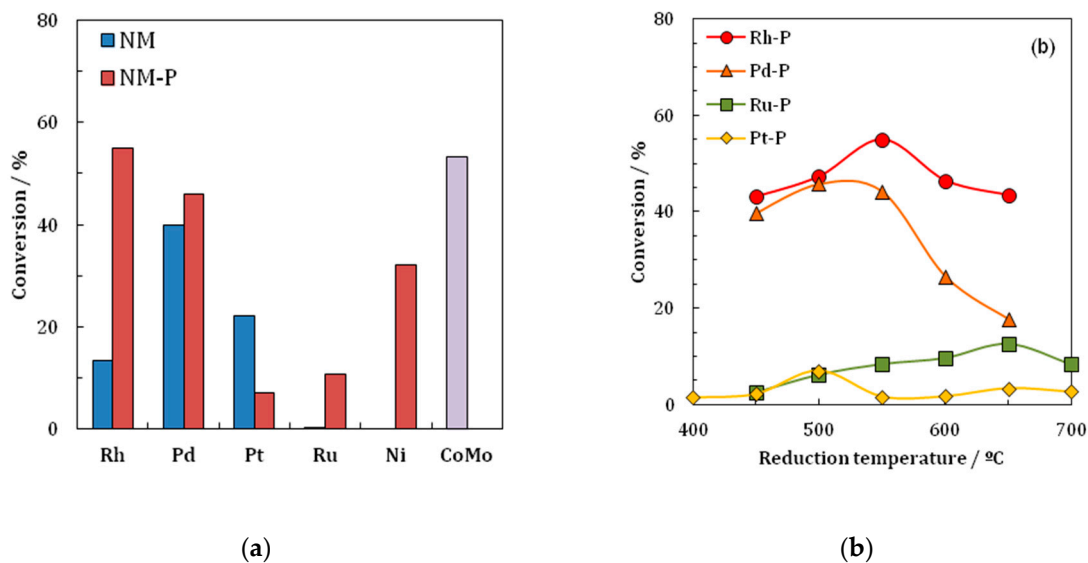


Figure 4. Results from the investigation of Kanda et al.: (a) Conversion values for the different catalyst materials reduced at optimal temperature; (b) Effect of the reduction temperature of the catalysts on the HDS conversion. Printed with permission of [29].

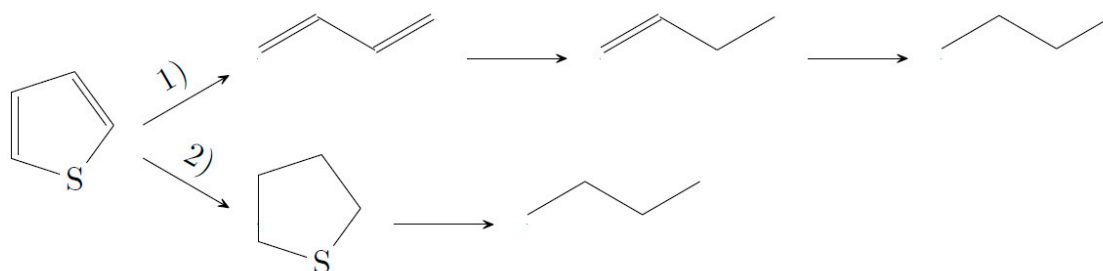


Figure 5. Reaction scheme for the possible pathways of the hydrodesulfurization (HDS) of thiophene with platinum group metal (PMG) phosphides [29].

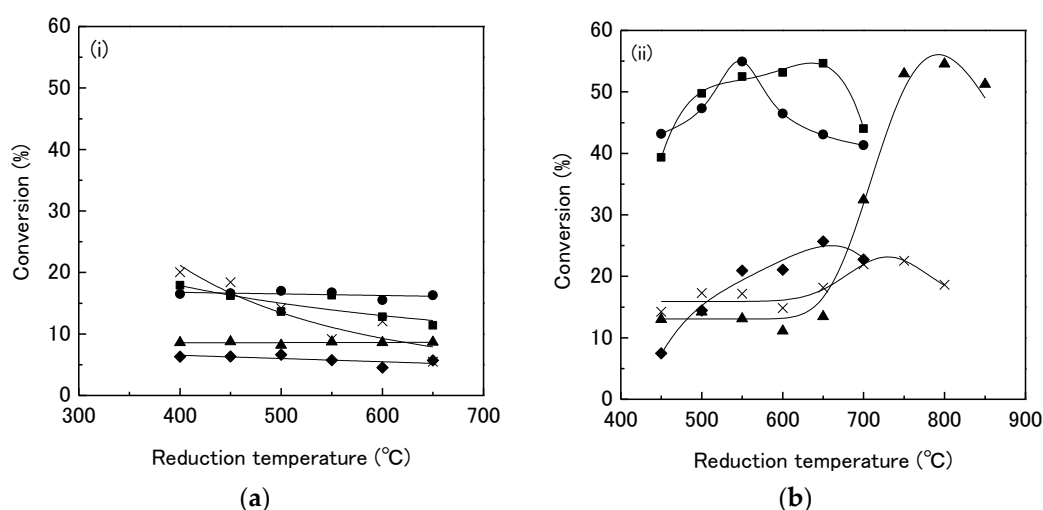
In a further publication [30], Kanda investigated the effect of the support material and reduction temperature on the performance of the Rh_2P catalysts on the HDS of thiophene. The activity of the sample changes with the support material. The catalysts on SiO_2 , Al_2O_3 , and TiO_2 are the most active followed by MgO and last ZrO_2 , as shown in Table 6. Further, as mentioned above, the results show that the formation of the phosphides enhances the activity of the materials, as Table 6 shows. The highest conversion value for a supported Rh catalyst material is 20.03% (Rh/ZrO_2), while the Rh_2P material supported on SiO_2 , Al_2O_3 , or TiO_2 reaches conversion values of approx. 54%. Further, TPR experiments show that the reduction behavior of the phosphate precursors to the phosphides changes with the support material, due probably to metal-support interactions. A reduction temperature as high as 800 °C is needed to convert the phosphate precursors to Rh_2P on Al_2O_3 , while the material on SiO_2 is converted to Rh_2P at a temperature of 550 °C. Last, the group investigated the effect of the reduction temperature. The materials are reduced at different temperatures in the range of 450–850 °C and their performance in the HDS of thiophene was compared. All materials show an increase in turnover frequency (TOF) with an increasing reduction temperature. The most significant increase is observed with the materials supported on Al_2O_3 (Table 7, Figure 6). The sample reduced at 450 °C displays a TOF of only 22.9 h^{-1} while the sample reduced at 850 °C shows a TOF of 251.4 h^{-1} . The increase in the TOF is due to the formation of Rh_2P at higher reduction temperatures, which is more active than Rh or the phosphate species.

Table 6. Effect of the support material on the performance of Rh₂P in the HDS of thiophene (fixed-bed reactor, 0.1 g catalyst, 350 °C, 0.1 MPa, H₂/thiophene = 30, W/F = 37.9 g h mol⁻¹) [30].

Catalyst	Support Material	Reduction Temperature [°C]	Conversion [%]	C ₁ -C ₃	Butanes	Butenes	1,3-Butadiene	THT ¹
Rh	SiO ₂	500	17.01	0.25	10.36	85.93	0.00	3.45
Rh	Al ₂ O ₃	450	8.75	1.86	14.71	82.17	0.00	1.26
Rh	TiO ₂	400	17.94	0.80	13.64	82.60	0.00	2.96
Rh	MgO	500	6.61	0.27	10.53	85.52	0.00	3.68
Rh	ZrO ₂	400	20.03	0.09	12.29	82.28	0.10	5.24
Rh ₂ P	SiO ₂	550	54.95	0.11	20.82	75.54	0.00	3.53
Rh ₂ P	Al ₂ O ₃	800	54.55	0.16	20.86	75.15	0.01	3.83
Rh ₂ P	TiO ₂	650	54.64	0.06	21.46	74.77	0.00	3.70
Rh ₂ P	MgO	650	25.67	0.00	11.45	82.87	0.00	5.66
Rh ₂ P	ZrO ₂	750	22.53	0.15	7.74	78.46	0.00	13.64

¹ THT: tetrahydrofuran.**Table 7.** Effect of the reduction temperature on the TOF of the Rh₂P catalyst materials in the HDS of thiophene (fixed-bed reactor, 0.1 g catalyst, 350 °C, 0.1 MPa, H₂/thiophene = 30, W/F = 37.9 g h mol⁻¹) [30].

Catalyst	Support	Reduction Temperature [°C]	TOF ¹ [h ⁻¹]
Rh ₂ P	SiO ₂	450	99.0
	SiO ₂	700	198.1
Rh ₂ P	Al ₂ O ₃	450	22.9
	Al ₂ O ₃	850	251.4
Rh ₂ P	TiO ₂	450	182.9
	TiO ₂	700	601.9
Rh ₂ P	MgO	450	15.2
	MgO	700	106.7
Rh ₂ P	ZrO ₂	450	350.5
	ZrO ₂	750	502.9

¹ TOF calculated from the CO uptake.**Figure 6.** Results from the investigations of Kanda et al. [30] on the effect of the reduction temperature on the conversion of thiophene: (a) Rh supported on different support materials; and (b) Rh₂P supported on different materials. Printed with permission of [30].

A further investigation by Kanda et al. [31] focused on the preparation of Rh₂P on SiO₂ and on the effect of the P loading and the reduction temperature on the HDS of thiophene. The highest HDS activity is observed on the catalyst with a loading of 5 wt % Rh and 1.5 wt % P on SiO₂, reduced at a temperature of 550 °C, which achieves conversion values of up to 55.0 % (Table 8) and a rate constant of approximately 21 mmol h⁻¹ g⁻¹. The higher activity of the 1.5 wt % P loaded catalyst is attributed to the formation of small Rh₂P particles at a relatively low reduction temperature (550 °C), as shown by the results from the TEM and PXRD investigations. The authors assumed that catalysts with lower P loadings (0.8 wt %) need higher temperatures for the formation of Rh₂P with Rh impurities and that high reduction temperatures lead to sintering of the active phase. Catalysts with higher P loadings (2.2–3.0 wt %) show the formation of highly dispersed Rh₂P already at lower temperatures (350 °C), but the excess P covers the active phase. A moderate P loading of 1.5 wt % leads to the formation of well-dispersed Rh₂P at moderate temperatures without the drawback of excess P covering or sintering due to the high reduction temperature.

Table 8. Effect of the P loading and reduction temperature on the performance of the Rh₂P/SiO₂ catalysts on the HDS of thiophene (fixed-bed reactor, 0.1 g catalyst, 350 °C, 0.1 MPa, H₂/thiophene = 30, W/F = 37.9 g h mol⁻¹) [31].

Catalyst	Support Material	Reduction Temperature [°C]	Conversion [%]	C ₁ –C ₃	Butanes	Butenes	THT ¹	TOF ² [h ⁻¹]
Rh	SiO ₂	550	16.8	0.3	9.9	86.4	3.3	21
Rh-0.8P	SiO ₂	550	27.9	0.0	15.8	81.2	3.0	50
Rh-1.5P	SiO ₂	450	43.2	0.3	22.0	74.5	3.4	137
Rh-1.5P	SiO ₂	550	55.0	0.1	20.8	75.6	3.5	202
Rh-1.5P	SiO ₂	650	43.1	0.1	14.4	81.0	4.3	230
Rh-2.2P	SiO ₂	550	45.4	0.2	21.4	72.6	5.9	312
Rh-3.0P	SiO ₂	550	14.2	0.4	9.9	72.4	17.3	147

¹ THT: tetrahydrofuran; ² TOF calculated from the CO uptake.

Sawanda et al. [33,34] investigated the HDS of thiophene with Rh₂P supported on zeolites. In the first investigation [10,33] the effect of adding Na to the Rh₂P catalysts supported on MFI zeolite, SiO₂, and Al₂O₃ on the HDS of thiophene was studied. The addition of Na to the zeolites increases the activity of the catalysts. The Rh₂P catalyst supported on NaMFI is higher than the catalysts supported on HMFI. The highest conversion values for the NaMFI catalyst is ca. 40% (Figure 7), while the HMFI reaches a maximum conversion value of ca 25% under identical conditions (fixed-bed reactor, 0.1 g catalyst, 350 °C, 0.1 MPa, H₂/thiophene = 30, W/F = 37.9 g h mol⁻¹). Sawanda suggested that the addition of Na decreases the interaction between the Al and the phosphate and thus enhances the reducibility of the phosphate species to Rh₂P and increases the activity of the catalysts. In a subsequent investigation [34], different Na-form zeolites (Na-beta, NaMFI, NaMOR) were used as supports for the Rh₂P catalyst and tested in the HDS of thiophene. The order of the thiophene conversion values is NaMFI (~35%) > Na-beta (~17%) » NaMOR (~8%) under identical reaction conditions (fixed-bed reactor, 0.1 g catalyst, 350 °C, 0.1 MPa, H₂/thiophene = 30, W/F = 37.9 g h mol⁻¹). Sawanda et al. attributed the low activity of NaMOR supported Rh₂P catalyst to the one-dimensional channel structure of NaMOR, so that the Rh and phosphate species do not easily diffuse into the micropores of the support material, leading to low CO uptake values and low catalyst activity. The catalyst supported on NaMOR displays CO uptake values between 2 and 7 μmol/g while the catalysts supported on NaMFI and Na-beta achieve CO uptake values as high as 40 μmol/g. Further, a significantly higher reduction temperature is needed for the formation of phase-pure Rh₂P supported on the Na-beta zeolite. Due to the high reduction temperature (850 °C), the structure of the support partially collapses, leading to lower activity of the Rh₂P/Na-beta catalyst.

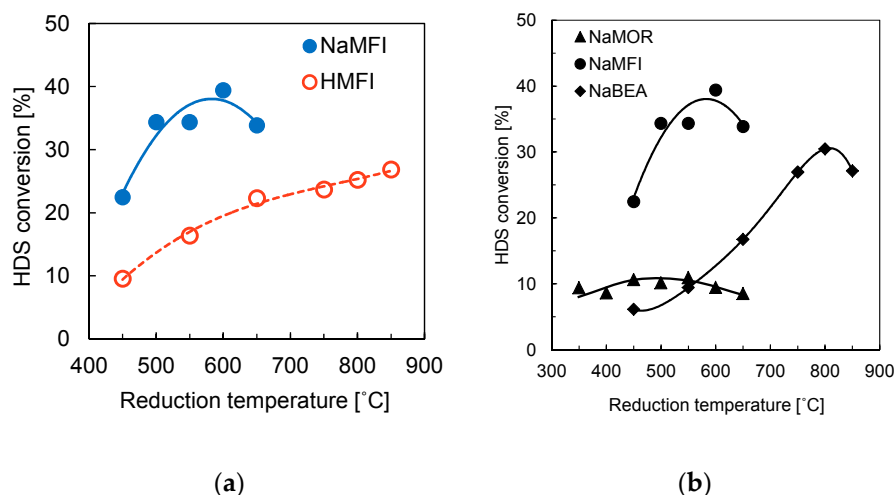


Figure 7. Effect of the reduction temperature and zeolite type on the HDS conversion of thiophene: (a) Effect of the addition of Na to the zeolite (Printed with the permission of ([33]; Copy right Elsevier); (b) Different types of zeolites (printed with permission of [34]).

Finally, Kanda compared the performance of two $\text{Rh}_2\text{P}/\text{Al}_2\text{O}_3$ catalysts prepared over two different pathways, the reduction of a supported phosphate precursor, and the conversion of supported Rh particles with TPP. The use of TPP reduces the reduction temperature from 800 to 450 °C for the formation of Rh_2P on Al_2O_3 . The highest conversion values in the HDS of thiophene (fixed-bed reactor, 0.1 g catalyst, 350 °C, 0.1 MPa, $\text{H}_2/\text{thiophene} = 30$, $W/F = 37.9 \text{ g h mol}^{-1}$) are achieved with catalysts prepared with TPP and reduced at 650 °C (the catalyst achieves a reaction rate of $38.5 \text{ mmol g}^{-1} \text{ h}^{-1}$, while the catalyst prepared over the phosphate reduction pathway achieves a reaction rate of $20.9 \text{ mmol g}^{-1} \text{ h}^{-1}$). At a reduction temperature of 450 °C, an excess of P covers the Rh_2P surface, which decreases the HDS activity of the catalysts. A reduction temperature of 650 °C eliminates the P excess and enhances the crystallinity of the Rh_2P nanoparticles and so increases the activity of the HDS. The higher activity of the catalysts prepared with TPP is attributed to the significantly smaller Rh_2P nanoparticles that have an average particle diameter of approx. 1.2 nm, while the particles prepared over the reduction of the phosphates have an average particle diameter of ca. 8.5 nm, according to the TEM studies performed in the investigation.

The investigations performed by Kanda and Sawanda and other research groups on the performance of supported Rh_2P catalysts and other supported noble metal phosphides as hydrotreating catalysts were reviewed in 2015 by Kanda and Uemichi [52].

4.2. Rh_2P as a Catalyst Material for HDO

In the last decades, transition metal phosphides have gained a lot of attention in hydroprocessing with the main focus on HDS [25,56]. PGM phosphides for HDO have only recently come into focus [24,25,57], also due to the emerging perspective of renewable resources for the production of fuels and chemicals. The most investigated phosphides in this field are non-noble metal phosphides such as Ni_2P , MoP , and Co_2P [56], and only recently Rh_2P and RuP have been considered as viable candidates.

Hydrodeoxygenation is a reaction that can be applied to different feeds and the specific process will determine the choice of the appropriate catalyst. Typically, HDO occurs parallel to HDS and HDN during hydrotreatment of conventional petroleum fractions. The oxygen content of most petroleum feedstocks is usually lower than 2% and sulfides of $\text{CoMo}/\gamma\text{-Al}_2\text{O}_3$ or $\text{NiMo}/\gamma\text{-Al}_2\text{O}_3$ [58] are the conventional and validated catalysts employed in this case (reaction condition range 3–10 MPa H_2 pressure, 300–500 °C). Bio-oils derived from biomass have a completely different composition, being remarkable for their high oxygen content (usually up to 40%) and water content (usually up to 30%) [59]. In the case of bio-oils, efficient HDO is relevant to improve their stability, increase the

heating value, and decrease the viscosity [58]. However, conventional hydrotreating catalysts are usually not stable in the presence of feeds containing high oxygen content without an additional supply of a S source [58]. Up to now, the identification of optimal catalyst systems for HDO has been a challenging task and several solutions have been proposed and investigated. The main challenge for identifying an appropriate HDO catalyst is that a large versatility to convert different functional groups with different reactivity is demanded and stability under the corrosive reaction conditions is vital. Indeed, typical bio-oils are complex mixtures constituted of oxygenated components, such as phenolics, furans, ethers, carboxylic acids, aldehydes, ketones, and alcohols (an example of the reactivity scale for HDO is provided by Elliott [60]). Phenols [61] and dibenzofurans [62] are generally chosen as model compounds to discriminate and estimate the HDO reactivity of a given catalyst system since they are the least reactive compounds to HDO.

Transition metal phosphides are potential candidates in HDO. Especially, metal-rich phosphides that have excellent heat and electrical conductivities and high thermal and chemical stabilities can match the properties desired for hydrotreatment [25,54,63]. This can be attributed to their good hydrogen transfer properties that are enhanced by the presence of phosphorus [64,65].

As described in the case of Ni_2P , the presence of phosphorus has an important effect on the HDO activity [65,66]. Phosphorus has a ligand effect on the metal site of the phosphide, modifying the electron density on the metal cation ($\text{M}^{\delta+}$) and resulting in an easier hydrogen dissociation on this surface, and the catalytic center can act as a Lewis acid [55,66]. The group P–OH, which is co-located on the metal phosphide phase as result of an incomplete reduction of phosphorus on the surface, constitutes a Brønsted acid of moderate acidity [63,66]. The synergy between the two groups (metallic and acidic) promotes catalyst activity comparable to that of a noble metal on an acidic support material and can be described as a cooperative mechanism over more than one neighboring catalytic center. The metal centers are active for hydrogenation, hydrogenolysis, and demethylation reactions [66], while PO–H groups can donate active hydrogen species as well, but they are much less active than the metal site. A higher d electron density of the metal is described as beneficial for an improved activity. A proposed HDO mechanism is reported in Figure 8. The oxygenated compounds and adsorbed H_2 are activated on the metal center and hydrogen atoms from the metal center and P–OH site react with the oxygenated species adsorbed on the surface; finally, water and the deoxygenated product species are formed [55].

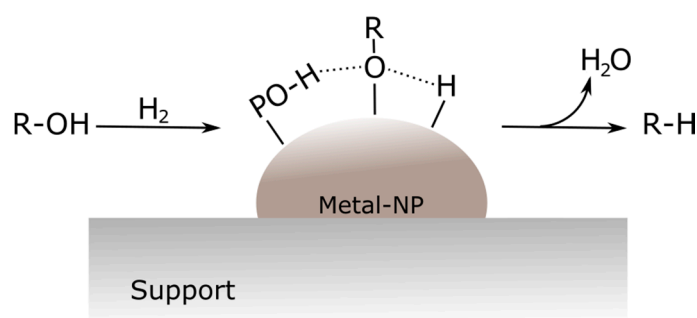
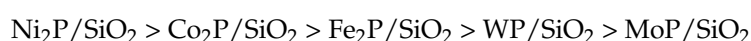


Figure 8. Proposed mechanism for HDO on a transition metal catalyst as described in Reference [66]; the graphics are redrawn according to the reference.

Ni_2P is one of the most studied metal phosphides for hydrotreatment showing good HDO activity as well for model compounds and biomass-derived feeds [57,61,67]. Zhao et al. [61] demonstrated that Ni_2P shows superior activity compared to other base metals. The following sequence in activity was reported for several phosphides in the HDO of guaiacol in a fixed-bed reactor at 300 °C and atmospheric pressure:



All the catalysts are less active than Pd/Al₂O₃, and the least stable system proved to be Co-MoS₂/Al₂O₃, representing an advantage of the phosphide materials. Another study related to phenol HDO underlines that phosphides can be active in hydrogenation as well as in isomerization [68]. For the phosphide materials, this results in higher selectivity for methylcyclopentane than cyclohexane during conversion of phenol. Koike et al. [57] explored Ni₂P/SiO₂ in the HDO of bio-oil produced from cedar chips in a two-stage fluidized bed reactor (0.1 MPa, 300 °C and 350 °C, residence time 0.64–1.0 s). Phenolic compounds were unreactive under the reaction condition used and a lower deoxygenation degree was recorded compared to the test with 2-methyltetrahydrofuran as the model compound.

Rh₂P has received less attention than Ni₂P but recent studies have demonstrated a high activity in HDO, superior also to that of supported noble metals in metallic form [25,47]. Griffin et al. [47] employed Rh₂P nanoparticles, obtained via solution-phase synthesis, supported on silica for guaiacol HDO. The catalytic tests were carried out in a reactor system allowing continuous flow at 350 °C, 0.5 MPa with a ratio 12:1 H₂ to guaiacol, and WHSV 5 h⁻¹. The synthesis method of the catalyst has an influence on the catalytic performance; a better selectivity towards deoxygenated species has been found for nanoparticles synthesized in solution-phase compared to incipient wetness (IW) impregnation (Figure 9). The activity of Rh₂P/SiO₂ in guaiacol conversion is not the highest among the tested catalysts but it has the highest selectivity for deoxygenated products such as cyclohexane and benzene (26% combined). Compared to the other catalysts (such as Rh/SiO₂, Ni/SiO₂, Ni₂P/SiO₂), Rh₂P/SiO₂ is more selective for C–O cleavage of the aryl–OH bond, giving benzene and anisole as the products.

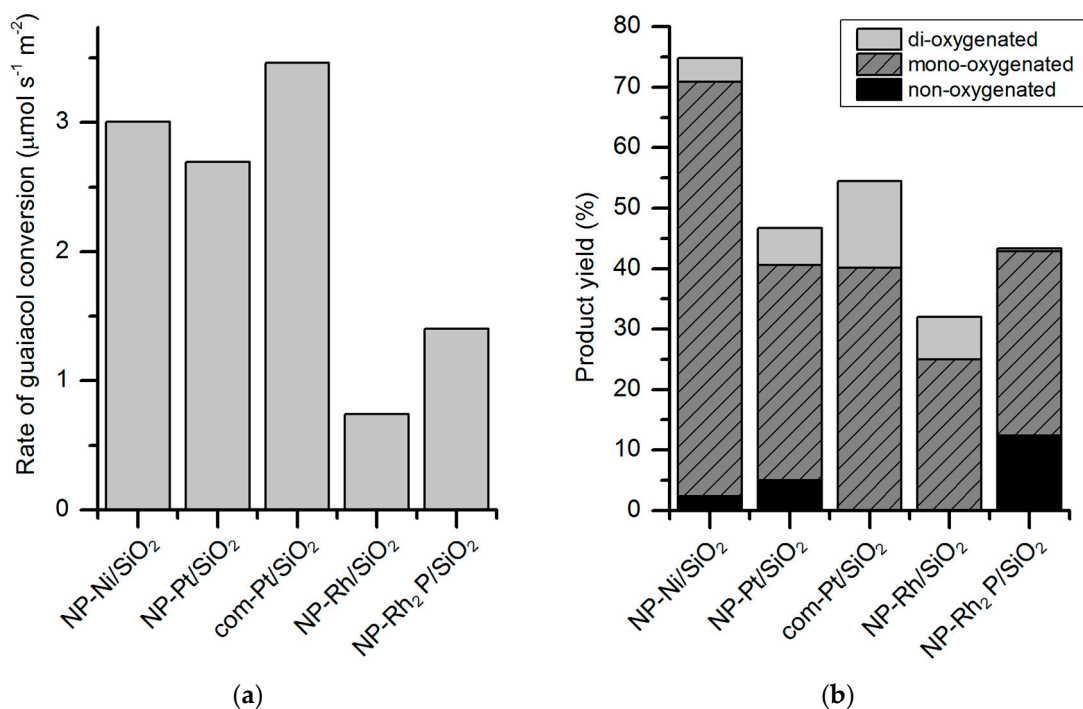


Figure 9. (a) Conversion rate normalized per square meter (m²) of active phase surface area observed during the hydrodeoxygenation of guaiacol; (b) Product yield of non-, mono- and di-oxygenated species from guaiacol HDO. “NP” is for nanoparticles, “com” for commercial. Reaction conditions: 350 °C, 0.5 MPa, 12 H₂:1 guaiacol, WHSV 5 h⁻¹. Graphics are redrawn according to Reference [47].

Further studies on Rh₂P on different support materials were also carried out by Griffin et al. [69]. Similar reaction conditions compared to the previous study [47] were used with Rh₂P on TiO₂, Al₂O₃, and MgO as support materials in order to assess the influence of the support in HDO of guaiacol as the model compound. Rh₂P/TiO₂ and Ni/TiO₂ exhibit higher guaiacol conversion showing products

with lower O:C ratio for C₅₊ fraction compared to the catalysts supported on active carbon. This is attributed to the properties of TiO₂, which displays reducible oxygen vacancies capable of facilitating C–O bond scission without aromatic ring hydrogenation. Ni/Al₂O₃ and Rh₂P/Al₂O₃ have also been found to be highly active catalysts, but they are less selective toward deoxygenation, and they also promote alkylation. MgO as support material produces the worst performance among the catalyst set investigated; it is speculated that the basic nature of the support is the main reason for the observation.

Habas et al. [28] investigated the activity of Ni₂P, Rh₂P, and Pd₃P on the HDO of acetic acid in a temperature range from 200 to 500 °C. The metal phosphide nanoparticles were synthesized by commercially available, air-stable metal–phosphine complexes in a one-pot reaction and supported on silica. Analogous catalysts were prepared by incipient wetness as a comparison. Both Rh₂P and Ni₂P show hydrogen-assisted decarbonylation reactions with CO, CH₄, and H₂O as products. Pd₃P does not show remarkable activity.

Cecilia et al. [38] were able to enhance the catalyst activity of Ni₂P by adding Rh, Ru, Ir, and Pt (molar ratio metal/Ni = 10%). The catalyst activity for HDO of dibenzofuran (P = 3.0 MPa, 175–300 °C, fixed-bed reactor) follows the sequence:



The structural interaction between the phosphide Ni₂P and the noble metal was not clarified but it was observed that Rh, Ru, and Ir could effectively enhance the catalyst activity and stability, while Pt provokes the opposite effect. The presence of a noble metal seems to improve the adsorption and activation of hydrogen in the metal support interface and it increases the presence of P–OH.

Bowker et al. [70] described the synthesis and HDO activity of silica-supported ruthenium phosphide (Ru₂P, RuP) catalysts. At 400 °C in a continuous reactor, Ru₂P and RuP are more active in HDO of furan than the conventional CoMo/Al₂O₃ catalyst, as reported in the sequence:



Ru₂P/SiO₂ is the most active and stable catalyst of the set (TOS 48 h). Higher selectivity for C₄ hydrocarbons is attributed to the presence of phosphorus, compared to Ru metal that produces more C₃ compounds.

One of the biggest dilemmas concerning transition metal phosphides is their stability in contact with complex mixtures such as petroleum fractions or real bio-oils in the process reaction conditions. Only a few studies have reported the stability of these catalysts and offer insight into the eventual deactivation processes of these catalysts. Typically, water created in the reaction or present initially in the feed can deactivate or degrade the catalyst through the formation of phosphates or the respective metal oxides from the corresponding phosphides [66]. Griffin et al. [69] reported that metal phosphides show a tolerance to water under the acidic conditions present in pyrolysis vapors. Cecilia et al. [62] asserted that Ni₂P shows high resistance to deactivation towards coke, although the water produced as a byproduct could be responsible for the slight decrease in activity. Koike et al. [57] identified coke formation as the main source of deactivation for Ni₂P/SiO₂. Griffin et al. [69] reported also for Rh₂P an increase in the coke deposited on the catalyst surface during guaiacol HDO.

In conclusion, metal phosphides appear promising for HDO although their activity may be lower compared to their intrinsic activity in HDS or HDN. The advantage of these materials is that their properties can be tuned depending on the metal chosen or by varying the metal/phosphorus ratio or the particle size of the phosphides [54]. It will be interesting to see the advances in the field in order to design an optimal phosphide-based catalyst for HDO.

4.3. Other Successful Examples of Catalysis with Rh₂P

The homogeneously catalyzed hydroformylation of olefins is one of the most important large-scale industrial processes. Cobalt carbonyl complex-based catalyst systems are still used today for the

hydroformylation of mid- and long-chain olefins, while the inherently more active rhodium carbonyl complexes stabilized with phosphine or phosphite ligands are applied for the hydroformylation of short olefins. The application of expensive rhodium catalyst systems demands an effective separation of the catalyst from the reaction products to minimize the risk of rhodium loss and catalyst deactivation. This explains why rhodium is only applied for the hydroformylation of short olefins where the separation of the products by distillation is feasible or alternatively the biphasic process where the catalyst complex remains in the aqueous phase while the products are removed over the organic phase.

Technical solutions involving heterogeneous catalysts in the hydroformylation with the catalyst in the solid phase and the products in the gas or liquid phase could offer alternatives that may also lead to new solutions regarding the process design. Research activities in academia and in industry are focusing on the synthesis and development of heterogeneous or heterogenized molecular hydroformylation catalysts that have proven to be inferior to the current state of the art in homogeneous catalysis [71–75].

As shown in the previous section, PGM phosphides, and especially rhodium phosphide, have proven to be useful heterogeneous catalysts for hydrotreating reactions. Although the phosphides show high catalytic activity in different reactions, they have not been widely considered as candidates in reactions involving the activation of carbon monoxide such as the hydroformylation of lower olefins.

We have carried out tests with Rh_2P on SiO_2 as a catalyst for the gas phase hydroformylation of ethylene and propylene [35]. The preparation of these catalysts was carried out via the incipient wetness impregnation of phosphate precursors followed by a reductive thermal treatment at different temperatures. The samples show the formation of phase-pure Rh_2P particles on SiO_2 at a reduction temperature of 500 °C, as PXRD investigation illustrated; highly crystalline Rh_2P nano-particles could be retained even at a reduction temperature of 900 °C, as proven by HRTEM investigations.

The samples were tested in a fixed-bed reactor system for the gas phase hydroformylation of ethylene, where the best results are achieved at low H_2/CO ratios (50 bar; GHSV = 2773 h^{-1} ; 170–240 °C; 10% C_2H_4 ; 10% H_2 ; 70% CO ; 10% Ar). A further increase in the selectivity of the catalysts towards the aldehyde is observed when water is added to the feed. It is reasoned that by adding water to the system the formation of the hydrogenation product ethane and the aldol condensation of the aldehyde are suppressed so that the selectivity of the desired aldehyde increases.

A comparison between the performance of the catalysts reduced at different temperatures has proven that the most active and selective catalysts are the catalyst types reduced at the highest temperatures. Such catalysts are highly stable: the spent catalyst of the sample reduced at 900 °C displays phase-pure Rh_2P on SiO_2 . Further evidence to rationalize the higher activity of the catalyst reduced at 900 °C can be taken from the IR absorption spectra after CO adsorption. The IR spectra of the catalyst reduced at 500 °C shows different signals in the region around 2000 cm^{-1} that correspond to both the linearly and bridged bonded CO on Rh atoms. The sample reduced at 900 °C shows only one signal at 2700 cm^{-1} , which corresponds to the CO linearly bonded to the Rh atom, and which formation favors the hydroformylation of the olefin as reported by Chuang and Pien [73–75]. Considering these facts, the authors suggest that this finding can be taken as evidence that Rh_2P in the form of highly crystalline-supported nanoparticles features surface sites that allow catalytic functionality similar to that of a phosphine- or phosphite-modified rhodium complex [76].

Based on the results presented and the fact that single-site catalysis is the proposed mode of action for Rh_2P , the question may be raised as to what the nature of the catalytically active site is. From the evidence we have gathered [35,76] and the structural considerations, we can draw the following conclusions: Rh_2P crystallizes in the cubic CaF_2 phase prototype. The nano-particle catalysts are highly crystalline and one can take as first approximation the bulk structure as the model for potential surface terminations. The CO-adsorption experiments prove that the surface must be terminated with exposed metal species. Cuts through the cubic CaF_2 phase prototype, even along high index surfaces, suggest that for all geometries separation of rhodium sites by phosphorus is obtained. In light of the fact that the spectroscopic data indicate that the presence of single rhodium sites available on highly crystalline

nano-particles is a prerequisite for good performance, we suggest that single-site catalysis is the mode of action relevant for the materials discussed. The rhodium sites are separated and coordinated by phosphorus and the prevailing motive of these solids can be summarized as “frustrated” single catalytic sites that do not cooperate, which is in contrast to the examples mentioned above in Rh₂P as hydroprocessing catalysis [76]. Although Rh₂P is present as an extended solid, the specific structure of the solid and the fact that a metal and a non-metal are the constituents do create an environment suitable for single site catalysis: the motif of “frustration” can be taken as the new descriptor for the development of alternative catalytic materials for single site catalysis.

Further, we also report the application of the catalysts in the hydroformylation of larger olefins, such as propylene, with a selectivity of 90% towards butyraldehyde with an n/iso ratio of 2.4 in the gaseous phase. Here again, a positive effect can be observed when water is added to the feed stream. Last, the catalysts are tested in the methoxycarbonylation of ethylene by exchanging hydrogen in the feed gas mixtures by methanol. Under the conditions applied, no ester formation could be observed. By adding small amounts of hydrogen, noticeable amounts of the product methyl propionate, together with major amounts of propionaldehyde and ethane, could be observed. From this observation, a reaction mechanism in which the ester is not formed via alkoxycarbonylation but via dehydrogenation of an intermediate hemiacetal is suggested.

5. Conclusions

Metal phosphides have been developed in the last years as hydrotreating catalysts. The reports show high activity of Ni₂P, MoP, and Rh₂P as catalysts for the reactions of HDS, HDN, and HDO. The development of the noble metal phosphide catalysts for hydrotreating catalysts shows that Rh₂P displays the highest activity in the HDS and HDO reactions. The main factors affecting the activity of Rh₂P are the preparation pathway and precursors, reduction temperature, and support material as shown by the broad investigations by Kanda et al. [29–34,43,52]. For deoxygenation reactions, cooperative mechanisms of multifunctional or adjacent sites are discussed as a major motive. Despite the high activity of the phosphides in hydrotreating reactions, only one publication [35] was found regarding the application of phosphides in CO activation reactions, such as the hydroformylation of short olefins. Here, Rh₂P appears to be an active, stable catalyst for the hydroformylation of short olefins. The characterization of the catalysts via XRD, TEM, and DRIFTS suggests that the highly crystalline Rh₂P nanoparticles on the support material features surface sites with a catalytic functionality similar to that of a phosphine- or phosphite-modified rhodium complex, which can be described as single-site catalysis or “frustrated” catalytic sites. This review gives an overview of the versatility of Rh₂P and its applications in heterogeneous catalyst systems. Here it shows high activity not only in hydrotreating reactions but also in CO activation reactions, such as the hydroformylation, expanding the possible applications of Rh₂P as a catalyst material.

Conflicts of Interest: The authors declare no conflict of interest.

References

1. Pöttgen, R.; Hönlé, W.; von Schnering, H.G. Phosphides: Solid-State Chemistry. In *Encyclopedia of Inorganic and Bioinorganic Chemistry*; John Wiley & Sons, Ltd.: Hoboken, NJ, USA, 2011; ISBN 978-1-119-95143-8.
2. Kuz'ma, Y.; Chykhrij, S. Chapter 156 Phosphides. In *Handbook on the Physics and Chemistry of Rare Earths*; Elsevier: Amsterdam, The Netherlands, 1996; Volume 23, pp. 285–434.
3. Aronsson, B.; Lundström, T.; Rundqvist, S. *Borides, Silicides and Phosphides: A Critical Review of Their Preparation, Properties and Crystal Chemistry*; Methuen Publishing: London, UK, 1965.
4. Kjekshus, A. Properties of binary compounds with the CoSb₂ type crystal structure. *Acta Chem. Scand.* **1971**, *25*, 411–422. [[CrossRef](#)]
5. Rundqvist, S. Phosphides of the B31 (MnP) structure type. *Acta Chem. Scand.* **1962**, *16*, 287–292. [[CrossRef](#)]
6. Andersson, Y. The crystal structure of palladium phosphide (Pd₁₅P₂). *ChemInform* **1977**, *31*, 355–358.

7. Andersson, Y.; Rundqvist, S.; Tellgren, R.; Thomas, J.O.; Flanagan, T.B. Neutron powder diffraction investigation of pure and deuterated palladium phosphide Pd₆P. *Acta Crystallogr. B* **1981**, *37*, 1965–1972. [[CrossRef](#)]
8. Holseth, H.; Kjekshus, A.; Andresen, A.F. Compounds with the marcasite type crystal structure. *Acta Chem. Scand.* **1968**, *22*, 3273–3283. [[CrossRef](#)]
9. Wiehage, G.; Weibke, F.; Blitz, W.; Meisel, K.; Wiechmann, F. Beiträge zur systematischen Verwandtschaftslehre. 70. Über das Vereinigungsvermögen von Palladium und Phosphor. *Z. Anorg. Allg. Chem.* **1936**, *228*, 357–371. [[CrossRef](#)]
10. Zachariasen, W.H. The crystal structure of palladium diphosphide. *Acta Crystallogr.* **1963**, *16*, 1253–1255. [[CrossRef](#)]
11. Gullman, L.-O. X-ray diffraction and thermo-analytical investigation of the palladium-phosphorus system. *J. Common Met.* **1966**, *11*, 157–167. [[CrossRef](#)]
12. Dahl, E. Refined crystal structures of PtP₂ and FeP₂. *Acta Chem. Scand.* **1969**, *23*, 2677–2684. [[CrossRef](#)]
13. Rundqvist, S. Phosphides of the platinum metals. *Nature* **1960**, *185*, 31. [[CrossRef](#)]
14. Dahl, E. The Crystal Structure of Pt₅P₂. *Acta Chem. Scand.* **1967**, *21*, 1131–1137. [[CrossRef](#)]
15. Matković, T.; Schubert, K. Kristallstruktur von Pd₇P₃. *J. Common Met.* **1977**, *55*, 177–184. [[CrossRef](#)]
16. Rundqvist, S. The structures of Co₂P, Ru₂P and related phases. *Acta Chem. Scand.* **1960**, *14*, 1961–1979. [[CrossRef](#)]
17. Hönle, W.; Kremer, R.; von Schnering, H.G. Ruthenium (III) triphosphide RuP₃: Preparation, crystal structure and properties. *Z. Krist. Cryst. Mater.* **1987**, *179*, 443–454. [[CrossRef](#)]
18. Zumbusch, M. Über die Strukturen des Uransubsulfids und der Subphosphide des Iridiums und Rhodiums. *Z. Anorg. Allg. Chem.* **1940**, *243*, 322–329. [[CrossRef](#)]
19. Flörke, U.; Jeitschko, W. Preparation and properties of new modifications of RuP₄ and OsP₄ with CdP₄-type structure. *J. Common Met.* **1982**, *86*, 247–253. [[CrossRef](#)]
20. El Ghadraoui, E.H.; Guerin, R.; Sergent, M. Diphosphure de trirhodium, Rh₃P₂: Premier exemple d'une structure lacunaire ordonnée de type anti-PbFCl. *Acta Crystallogr. C* **1983**, *39*, 1493–1494. [[CrossRef](#)]
21. Rundqvist, S.; Hede, A. X-Ray Investigation on Rhodium Phosphides. The Crystal Structure of Rh₄P₃. *Acta Chem. Scand.* **1960**, *14*, 893–902. [[CrossRef](#)]
22. Furuseth, S.; Selte, K.; Kjekshus, A.; Nielsen, P.H.; Sjöberg, B.; Larsen, E. Redetermined Crystal Structures of PdAs₂, PdSb₂, PtP₂, PtAs₂, PtSb₂, a-PtBi₂, and AuSb₂. *Acta Chem. Scand.* **1965**, *19*, 735–741. [[CrossRef](#)]
23. Okamoto, H. The P-Rh (phosphorus-rhodium) system. *Bull. Alloy Phase Diagr.* **1990**, *11*, 415–417. [[CrossRef](#)]
24. Prins, R.; Bussell, M.E. Metal phosphides: Preparation, characterization and catalytic reactivity. *Catal. Lett.* **2012**, *142*, 1413–1436. [[CrossRef](#)]
25. Oyama, S.T.; Gott, T.; Zhao, H.; Lee, Y.-K. Transition metal phosphide hydroprocessing catalysts: A review. *Catal. Today* **2009**, *143*, 94–107. [[CrossRef](#)]
26. Oyama, S.T. Transition metal carbides, nitrides, and phosphides. In *Handbook of Heterogeneous Catalysis*; John Wiley & Sons, Ltd.: Hoboken, NJ, USA, 2008.
27. Hayes, J.R.; Bowker, R.H.; Gaudette, A.F.; Smith, M.C.; Moak, C.E.; Nam, C.Y.; Pratum, T.K.; Bussell, M.E. Hydrodesulfurization properties of rhodium phosphide: Comparison with rhodium metal and sulfide catalysts. *J. Catal.* **2010**, *276*, 249–258. [[CrossRef](#)]
28. Habas, S.E.; Baddour, F.G.; Ruddy, D.A.; Nash, C.P.; Wang, J.; Pan, M.; Hensley, J.E.; Schaidle, J.A. A facile molecular precursor route to metal phosphide nanoparticles and their evaluation as hydrodeoxygenation catalysts. *Chem. Mater.* **2015**, *27*, 7580–7592. [[CrossRef](#)]
29. Kanda, Y.; Temma, C.; Nakata, K.; Kobayashi, T.; Sugioka, M.; Uemichi, Y. Preparation and performance of noble metal phosphides supported on silica as new hydrodesulfurization catalysts. *Appl. Catal. Gen.* **2010**, *386*, 171–178. [[CrossRef](#)]
30. Kanda, Y.; Nakata, K.; Temma, C.; Sugioka, M.; Uemichi, Y. Effects of Support on Formation of Active Sites and Hydrodesulfurization Activity of Rhodium Phosphide Catalyst. *J. Jpn. Pet. Inst.* **2012**, *55*, 108–119. [[CrossRef](#)]
31. Kanda, Y.; Temma, C.; Sawada, A.; Sugioka, M.; Uemichi, Y. Formation of active sites and hydrodesulfurization activity of rhodium phosphide catalyst: Effect of reduction temperature and phosphorus loading. *Appl. Catal. Gen.* **2014**, *475*, 410–419. [[CrossRef](#)]

32. Kanda, Y.; Ichiki, T.; Kayaoka, S.; Sawada, A.; Sugioka, M.; Uemichi, Y. Preparation of Highly Active Noble Metal Phosphide Catalysts: Effect of Precursors on the Formation of the Active Phase and Hydrodesulfurization Activity. *Chem. Lett.* **2013**, *42*, 404–406. [[CrossRef](#)]
33. Sawada, A.; Kanda, Y.; Sugioka, M.; Uemichi, Y. Rhodium phosphide catalyst for hydrodesulfurization: Low temperature synthesis by sodium addition. *Catal. Commun.* **2014**, *56*, 60–64. [[CrossRef](#)]
34. Sawada, A.; Kanda, Y.; Sugioka, M.; Uemichi, Y. Formation of Rh₂P supported on Na-form and catalytic activity for hydrodesulfurization. *J. Jpn. Pet. Inst.* **2015**, *58*, 312–320. [[CrossRef](#)]
35. Alvarado Rupflin, L.; Mormul, J.; Lejkowski, M.; Titlbach, S.; Papp, R.; Gläser, R.; Dimitrakopoulou, M.; Huang, X.; Trunschke, A.; Willinger, M.G. Platinum group metal phosphides as heterogeneous catalysts for the gas-phase hydroformylation of small olefins. *ACS Catal.* **2017**, *7*, 3584–3590. [[CrossRef](#)]
36. Guan, Q.; Sun, C.; Li, R.; Li, W. The synthesis and investigation of ruthenium phosphide catalysts. *Catal. Commun.* **2011**, *14*, 114–117. [[CrossRef](#)]
37. Wang, Q.; Wang, Z.; Yin, X.; Zhou, L.; Zhang, M. A new approach to synthesize supported ruthenium phosphides for hydrodesulfurization. *Mater. Res. Bull.* **2016**, *74*, 98–102. [[CrossRef](#)]
38. Cecilia, J.A.; Infantes-Molina, A.; Sanmartín-Donoso, J.; Rodríguez-Aguado, E.; Ballesteros-Plata, D.; Rodríguez-Castellón, E. Enhanced HDO activity of Ni₂P promoted with noble metals. *Catal. Sci. Technol.* **2016**, *6*, 7323–7333. [[CrossRef](#)]
39. Yao, Y.; Tian, Y.-J.; Wu, H.-H.; Lu, S.-X. Pt-promoted and H β zeolite-supported Ni₂P catalysts for hydroisomerisation of n-heptane. *Fuel Process. Technol.* **2015**, *133*, 146–151. [[CrossRef](#)]
40. Muetterties, E.L.; Sauer, J.C. Catalytic properties of metal phosphides. Qualitative assay of catalytic properties. *J. Am. Chem. Soc.* **1974**, *96*, 3410–3415. [[CrossRef](#)]
41. Bowker, R.H.; Smith, M.C.; Carrillo, B.A.; Bussell, M.E. Synthesis and hydrodesulfurization properties of noble metal phosphides: Ruthenium and palladium. *Top. Catal.* **2012**, *55*, 999–1009. [[CrossRef](#)]
42. Kucernak, A.R.; Fahy, K.F.; Sundaram, V.N. Facile synthesis of palladium phosphide electrocatalysts and their activity for the hydrogen oxidation, hydrogen evolutions, oxygen reduction and formic acid oxidation reactions. *Catal. Today* **2016**, *262*, 48–56. [[CrossRef](#)]
43. Kanda, Y.; Matsukura, Y.; Sawada, A.; Sugioka, M.; Uemichi, Y. Low-temperature synthesis of rhodium phosphide on alumina and investigation of its catalytic activity toward the hydrodesulfurization of thiophene. *Appl. Catal. Gen.* **2016**, *515*, 25–31. [[CrossRef](#)]
44. Carencó, S.; Portehault, D.; Boissière, C.; Mezailles, N.; Sanchez, C. Nanoscaled metal borides and phosphides: Recent developments and perspectives. *Chem. Rev.* **2013**, *113*, 7981–8065. [[CrossRef](#)] [[PubMed](#)]
45. Henkes, A.E.; Schaak, R.E. Trioctylphosphine: A general phosphorus source for the low-temperature conversion of metals into metal phosphides. *Chem. Mater.* **2007**, *19*, 4234–4242. [[CrossRef](#)]
46. Henkes, A.E.; Schaak, R.E. Template-assisted synthesis of shape-controlled Rh₂P nanocrystals. *Inorg. Chem.* **2008**, *47*, 671–677. [[CrossRef](#)] [[PubMed](#)]
47. Griffin, M.B.; Baddour, F.G.; Habas, S.E.; Ruddy, D.A.; Schaidle, J.A. Evaluation of silica-supported metal and metal phosphide nanoparticle catalysts for the hydrodeoxygenation of guaiacol under ex situ catalytic fast pyrolysis conditions. *Top. Catal.* **2016**, *59*, 124–137. [[CrossRef](#)]
48. Cimino, S.; Lisi, L.; Mancino, G. Effect of phosphorous addition to Rh-supported catalysts for the dry reforming of methane. *Int. J. Hydrogen Energy* **2017**, *42*, 23587–23598. [[CrossRef](#)]
49. Oyama, S.T. Novel catalysts for advanced hydroprocessing: Transition metal phosphides—ScienceDirect. *J. Catal.* **2003**, *216*, 343–352. [[CrossRef](#)]
50. Wang, X.; Clark, P.; Oyama, S.T. Synthesis, Characterization, and Hydrotreating Activity of Several Iron Group Transition Metal Phosphides. *J. Catal.* **2002**, *208*, 321–331. [[CrossRef](#)]
51. Peroni, M.; Mancino, G.; Baráth, E.; Gutiérrez, O.Y.; Lercher, J.A. Bulk and γ -Al₂O₃-supported Ni₂P and MoP for hydrodeoxygenation of palmitic acid. *Appl. Catal. B Environ.* **2016**, *180*, 301–311. [[CrossRef](#)]
52. Kanda, Y.; Uemichi, Y. Noble Metal Phosphides as New Hydrotreating Catalysts: Highly Active Rhodium Phosphide Catalyst. *J. Jpn. Pet. Inst.* **2015**, *58*, 20–32. [[CrossRef](#)]
53. Song, L.; Li, T.; Zhang, S.; Zhang, S. Synthesis of rhodium phosphide cocatalyst and remarkably enhanced photocatalytic hydrogen evolution over CdS under visible light radiation. *Chem. Eng. J.* **2017**, *314*, 498–507. [[CrossRef](#)]

54. Boullosa-Eiras, S.; Lødeng, R.; Bergem, H.; Stöcker, M.; Hannevold, L.; Blekkan, E.A. Potential for metal-carbide, nitride, and phosphide as future hydrotreating (HT) catalysts for processing of bio-oils. In *Catalysis*; Royal Society of Chemistry: London, UK, 2014; pp. 29–71.
55. Arun, N.; Sharma, R.V.; Dalai, A.K. Green diesel synthesis by hydrodeoxygenation of bio-based feedstocks: Strategies for catalyst design and development. *Renew. Sustain. Energy Rev.* **2015**, *48*, 240–255. [[CrossRef](#)]
56. Lee, Y.-K.; Oyama, S.T. Sulfur resistant nature of Ni₂P catalyst in deep hydrodesulfurization. *Appl. Catal. Gen.* **2017**, *548*, 103–113. [[CrossRef](#)]
57. Koike, N.; Hosokai, S.; Takagaki, A.; Nishimura, S.; Kikuchi, R.; Ebitani, K.; Suzuki, Y.; Oyama, S.T. Upgrading of pyrolysis bio-oil using nickel phosphide catalysts. *J. Catal.* **2016**, *333*, 115–126. [[CrossRef](#)]
58. Mortensen, P.M.; Grunwaldt, J.-D.; Jensen, P.A.; Knudsen, K.G.; Jensen, A.D. A review of catalytic upgrading of bio-oil to engine fuels. *Appl. Catal. Gen.* **2011**, *407*, 1–19. [[CrossRef](#)]
59. Bridgwater, A.V. Review of fast pyrolysis of biomass and product upgrading. *Biomass Bioenergy* **2012**, *38*, 68–94. [[CrossRef](#)]
60. Elliott, D.C. Historical developments in hydroprocessing bio-oils. *Energy Fuels* **2007**, *21*, 1792–1815. [[CrossRef](#)]
61. Zhao, H.Y.; Li, D.; Bui, P.; Oyama, S.T. Hydrodeoxygenation of guaiacol as model compound for pyrolysis oil on transition metal phosphide hydroprocessing catalysts. *Appl. Catal. Gen.* **2011**, *391*, 305–310. [[CrossRef](#)]
62. Cecilia, J.A.; Infantes-Molina, A.; Rodríguez-Castellón, E.; Jiménez-López, A.; Oyama, S.T. Oxygen-removal of dibenzofuran as a model compound in biomass derived bio-oil on nickel phosphide catalysts: Role of phosphorus. *Appl. Catal. B Environ.* **2013**, *136*, 140–149. [[CrossRef](#)]
63. Berenguer, A.; Sankaranarayanan, T.M.; Gómez, G.; Moreno, I.; Coronado, J.M.; Pizarro, P.; Serrano, D.P. Evaluation of transition metal phosphides supported on ordered mesoporous materials as catalysts for phenol hydrodeoxygenation. *Green Chem.* **2016**, *18*, 1938–1951. [[CrossRef](#)]
64. Cecilia, J.A.; Infantes-Molina, A.; Rodríguez-Castellón, E.; Jiménez-López, A. A novel method for preparing an active nickel phosphide catalyst for HDS of dibenzothiophene. *J. Catal.* **2009**, *263*, 4–15. [[CrossRef](#)]
65. Oyama, S.T.; Wang, X.; Lee, Y.-K.; Bando, K.; Requejo, F.G. Effect of phosphorus content in nickel phosphide catalysts studied by XAFS and other techniques. *J. Catal.* **2002**, *210*, 207–217. [[CrossRef](#)]
66. He, Z.; Wang, X. Hydrodeoxygenation of model compounds and catalytic systems for pyrolysis bio-oils upgrading. *Catal. Sustain. Energy* **2012**, *1*, 28–52. [[CrossRef](#)]
67. Li, K.; Wang, R.; Chen, J. Hydrodeoxygenation of anisole over silica-supported Ni₂P, MoP, and NiMoP catalysts. *Energy Fuels* **2011**, *25*, 854–863. [[CrossRef](#)]
68. Boullosa-Eiras, S.; Lødeng, R.; Bergem, H.; Stöcker, M.; Hannevold, L.; Blekkan, E.A. Catalytic hydrodeoxygenation (HDO) of phenol over supported molybdenum carbide, nitride, phosphide and oxide catalysts. *Catal. Today* **2014**, *223*, 44–53. [[CrossRef](#)]
69. Griffin, M.B.; Baddour, F.G.; Habas, S.E.; Nash, C.P.; Ruddy, D.A.; Schaidle, J.A. An investigation into support cooperativity for the deoxygenation of guaiacol over nanoparticle Ni and Rh₂P. *Catal. Sci. Technol.* **2017**, *7*, 2954–2966. [[CrossRef](#)]
70. Bowker, R.H.; Smith, M.C.; Pease, M.L.; Slenkamp, K.M.; Kovarik, L.; Bussell, M.E. Synthesis and Hydrodeoxygenation Properties of Ruthenium Phosphide Catalysts. *ACS Catal.* **2011**, *1*, 917–922. [[CrossRef](#)]
71. Neves, Â.C.; Calvete, M.J.; Pinho e Melo, T.M.; Pereira, M.M. Immobilized catalysts for hydroformylation reactions: A versatile tool for aldehyde synthesis. *Eur. J. Org. Chem.* **2012**, *2012*, 6309–6320. [[CrossRef](#)]
72. Riisager, A.; Fehrmann, R.; Haumann, M.; Wasserscheid, P. Supported Ionic Liquid Phase (SILP) Catalysis: An Innovative Concept for Homogeneous Catalysis in Continuous Fixed-Bed Reactors. *Eur. J. Inorg. Chem.* **2006**, *2006*, 695–706. [[CrossRef](#)]
73. Chuang, S.S.; Pien, S.-I. Infrared spectroscopic studies of ethylene hydroformylation on Rh/SiO₂: An investigation of the relationships between homogeneous and heterogeneous hydroformylation. *J. Mol. Catal.* **1989**, *55*, 12–22. [[CrossRef](#)]
74. Chuang, S.S.; Pien, S.I. Infrared study of the CO insertion reaction on reduced, oxidized, and sulfided Rh/SiO₂ catalysts. *J. Catal.* **1992**, *135*, 618–634. [[CrossRef](#)]

75. Srinivas, G.; Chuang, S.S. An in-Situ Infrared Study of the Formation of n-and iso-Butyraldehyde from Propylene Hydroformylation on Rh/SiO₂ and Sulfided Rh/SiO₂. *J. Catal.* **1993**, *144*, 131–147. [[CrossRef](#)]
76. Schunk, S.A.; Alvarado Rupflin, L.; Mormul, J.; Lejkowski, M.; Titlbach, S.; Papp, R.; Gläser, R.; Dimitrakopoulou, M.; Huang, X.; Trunschke, A.; et al. New Horizons for Heterogeneously Catalyzed CO Insertion Reactions: From Molecular Sieves to Extended Complex Solids. In Proceedings of the Petrochemistry and Refining in a Changing Raw Materials Landscape DGMK Conference, Dresden, Germany, 9–11 October 2017.



© 2018 by the authors. Licensee MDPI, Basel, Switzerland. This article is an open access article distributed under the terms and conditions of the Creative Commons Attribution (CC BY) license (<http://creativecommons.org/licenses/by/4.0/>).